

reliability-constrained scenarios. Apart from high reliability and limited power consumption, the guarantee of low latency is also of profound significance to realize URLLC, while this topic was rarely examined except in a few existing works. Particularly, in [?], the age of information (AoI) was minimized for HARQ-IR-assisted multi-RIS systems while ensuring power and outage constraints. In addition, the authors in [?] maximized the overall rates of enhanced mobile broadband (eMBB) users in HARQ-assisted grant free systems under the constraint of a maximum tolerable probability of delay bound violation. However, independent fading channels were generally assumed in these works [?], [?], [?], [?], [?] whose results are inapplicable to the correlated fading channels. Due to the frequent occurrence of time-selective fading channels, there is an urgent need to propose a proper latency assurance strategy for HARQ schemes over correlated fading channels.

In order to minimize the delivery latency while guaranteeing the high reliability, this paper proposes a power-constrained HARQ strategy by considering time-correlated fading channels. The simple asymptotic outage expressions of HARQ schemes are adopted to avoid heavy computational burden. Unfortunately, the optimization problem still cannot be easily solved by using the off-the-shelf tools due to the fractional objective function and non-convex constraints. This has inspired us to explore the use of artificial intelligence (AI) techniques. By taking into account that the transmit power allocated in the current HARQ round is affected by the previous HARQ rounds regardless of the subsequent HARQ rounds, and the time correlation takes place among fading channels, it is natural to come up with graph neural networks to capture this special transmission structure. The graph convolutional network (GCN) is then invoked for the optimal power allocation of HARQ by treating different HARQ rounds and channel correlation as graph nodes and edges, respectively. The trainable GCN weights are updated by using [primal-dual learning approach](#). Finally, [latency and the reliability performance of the GCN-enabled power allocation strategy for the HARQ scheme](#) were investigated [through thorough numerical experiments](#), where [the three HARQ schemes include Type-I HARQ, CC HARQ, and HARQ-IR](#) but [at least](#), [despite its high coding complexity](#), HARQ-IR [provides the](#) lowest latency while ensuring reliable performance within strict power constraints.

The rest of the paper is structured as follows. Section ?? elaborates on the system model and formulates the latency minimization problem for power-constrained HARQ schemes. In Section ??, a GCN-enabled power allocation strategy is designed to solve the [optimization problem](#). Section ?? verifies the effectiveness of the proposed strategy through numerical experiments. Finally, concluding remarks are drawn in Section ??.

II. System Model

This paper considers a point-to-point HARQ-aided URLLC system. To begin, the system model is delineated in this section, including HARQ schemes, signal transmission model, and problem formulation.

A. HARQ Schemes

HARQ can be classified into three categories according to different coding operations, including Type-I HARQ, HARQ-CC, and HARQ-IR. More specifically, for both Type-I HARQ and HARQ-CC, the same codeword is delivered in all HARQ rounds. At the receiver side, Type-I HARQ decodes its message by solely relying on the currently received codeword, while HARQ-CC combines the erroneously received codewords for maximal-ratio combining (MRC). Undoubtedly, HARQ-CC outperforms Type-I HARQ due to the fact that even the failed packets contain useful information. Unlike Type-I HARQ and HARQ-CC, HARQ-IR transmits codewords with different redundancy among all HARQ rounds. Hence, a long codeword is first chopped into several sub-codewords at the transmitter, which will be sent one by one upon retransmission request. At the receiver, the previously received codewords are then concatenated to form a long codeword for the joint decoding. Owing to the high encoding/decoding complexity, HARQ-IR achieves the superior performance of reliability.

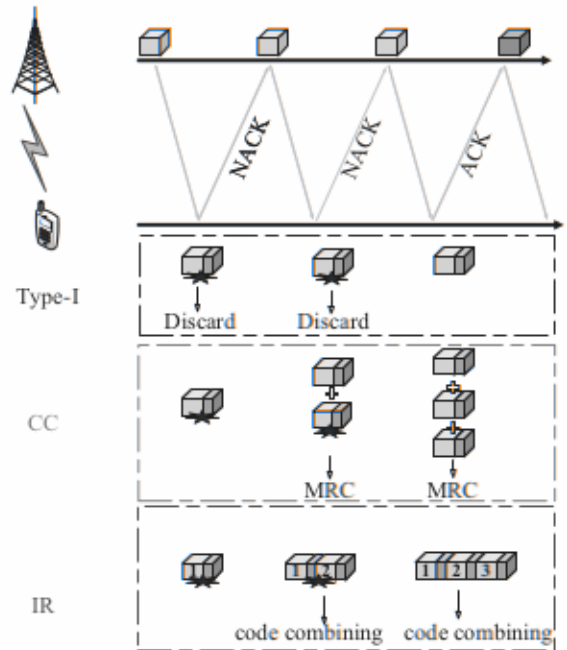


Fig. 1. An example of HARQ transmissions.

B. Signal Transmission Model

By considering blocking fading channels, the received signal in the k -th HARQ round can be expressed as

$$\mathbf{y}_k = h_k \mathbf{x}_k + \mathbf{n}_k, \quad (1)$$

It is noteworthy that GCN is suitable herein due to its ability of exploiting the graph structure to process data. In what follows, a GCN-enabled power allocation scheme is detailed.

A. GCN-Based Power Allocation

To enable the GCN-based power allocation, each HARQ round is modeled as a graph node. Moreover, as aforementioned that the statistical CSI is used, the graph edges can be characterized by the correlation coefficients among fading channels. More specifically, the channel correlation coefficient matrix \mathbf{H} is calculated as

$$\mathbf{H} = [\alpha_{ij}]_{1 \leq i, j \leq K}, \quad (11)$$

where the element α_{ij} is

$$\alpha_{ij} = \begin{cases} E\{h_i^* h_j\}, & i \leq j \\ 0, & \text{else} \end{cases}, \quad (12)$$

wherein the superscript $*$ denotes the complex conjugate operation and $E\{\cdot\}$ is the expectation operation. The rationale of $\alpha_{ij} = 0$ for $i > j$ is due to the fact the j -th HARQ round cannot be influenced by the i -th HARQ round. With the time-correlated channel model in (??), the diagonal entries of \mathbf{H} can be calculated as $E\{\|h_i\|^2\} = \xi_i^2$ and its off-diagonal entries are given by $E\{h_i^* h_j\} = \xi_i \xi_j \rho^{i+j+2\delta-2}$ [?]. Apparently, \mathbf{H} can be treated as the adjacency matrix in the directed graph network.

For tractability, the power policy functional space $\mathbf{p} = (p_1, p_2, \dots, p_K)$ is parameterized by using a graph neural networks. More specifically, the power allocation policy is defined as $\mathbf{p}(\mathbf{H}) = \Psi(\mathbf{H}; \mathbf{W})$, where Ψ represents a L -layer GCN with trainable weights \mathbf{W} . Instead of optimizing \mathbf{p} , the neural network parameters \mathbf{W} need to be optimally determined through the primal-dual learning approach [?]. As shown in Fig. ??, a L -layer GCN structure for the power-constrained HARQ schemes with $K = 5$ is given as an example. With the input $\mathbf{V}^{(0)} = \frac{\bar{p}}{K} \mathbf{1}_K$ to $\Psi(\mathbf{H}; \mathbf{W})$, the $(l+1)$ -th layer features $\mathbf{V}^{(l+1)}$ of GCN are updated by following the layer-wise propagation rule as

$$\mathbf{V}^{(l+1)} = \sigma_l \left(\mathbf{D}^{-\frac{1}{2}} \mathbf{H} \mathbf{D}^{-\frac{1}{2}} \mathbf{V}^{(l)} \mathbf{W}^{(l)} \right), \quad (13)$$

where $\mathbf{1}_K$ stands for an all-ones column vector, $\mathbf{D} = \text{diag}(\mathbf{H})$ denotes the degree matrix, $\mathbf{V}^{(l)} \in \mathbb{R}^{K \times n_l}$ is the matrix of node features in the l -th layer, $\mathbf{W}^{(l)} \in \mathbb{R}^{n_l \times n_{l+1}}$ is the trainable weight matrix in the l -th layer, $\sigma_l(\cdot)$ defines the activation function. Accordingly, the output of the L -th layer of the GCN is our desired power allocation policy.

B. Primal-Dual Learning Approach

In order to train the neural network weights \mathbf{W} , the iterative primal-dual learning approach is applied in this paper. Moreover, by realizing that the maximum allowable outage probability is generally very low (e.g., $\varepsilon = 10^{-2}$), we apply the logarithm transformation to the outage probability, i.e., $\log P_{out,K}$, in order to amplify the effect of the

outage constraint and meanwhile accelerate learning and alleviate the over-fitting. By taking this transformation into consideration, the Lagrangian of problem (??) is formulated as

$$\mathcal{L}_\Psi(\mathbf{W}, \lambda, v) = \tau + \lambda(\log P_{out,K} - \log \varepsilon) + v \left(\sum_{k=1}^K p_k P_{out,k-1} - \bar{p} \right), \quad (14)$$

where $\lambda \geq 0$ and $v \geq 0$ are the Lagrangian multiplier associated with the two constraints in problem (??). It is noteworthy that τ , $P_{out,K}$, and \mathbf{p} are the functions of the trainable parameters \mathbf{W} . According to the gradient descent algorithm, the neural network parameters \mathbf{W} at step s can be updated as

$$\mathbf{W}_{s+1} = \mathbf{W}_s - \theta_{\mathbf{W},s} \nabla_{\mathbf{W}} E_{\rho \sim \mathcal{A}} \{ \mathcal{L}(\mathbf{W}_s, \lambda_s, v_s) \}, \quad (15)$$

where the term $\theta_{\mathbf{W},s}$ denotes the step size at the s -th iteration and the actual time correlation ρ follows a certain distribution \mathcal{A} within the range $[0, 1)$. Besides, the multipliers are updated by capitalizing on the sub-gradient method as

$$\lambda_{s+1} = [\lambda_s + \theta_{\lambda,s} (E_{\rho \sim \mathcal{A}} \{ \log(P_{out,K}) \} - \log(\varepsilon))]_+, \quad (16)$$

$$v_{s+1} = [v_s + \theta_{v,s} (E_{\rho \sim \mathcal{A}} \{ p_{avg} \} - \bar{p})]_+, \quad (17)$$

where $\theta_{\lambda,s}$ and $\theta_{v,s}$ correspond to the step sizes, and $[x]_+ = \max\{0, x\}$. The pseudocode of GCN-based power allocation scheme is shown in Algorithm ??.

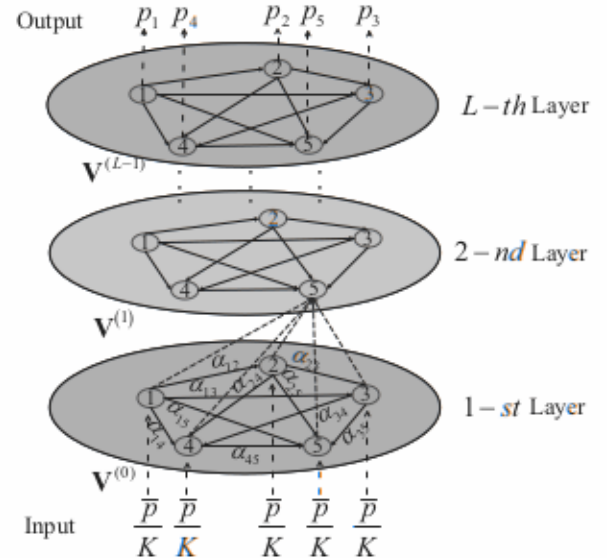


Fig. 2. A general L -layer GCN structure for the power-constrained HARQ schemes with $K = 5$.

Algorithm 1 GCN-Based Power Allocation Algorithm

 Input: Initial values \mathbf{W} , λ , v , $\mathbf{V}^{(0)}$

 Output: The power allocation policy $\mathbf{V}^{(L)}$;

- 1: for epoch $s = 1, 2, \dots$ do
 - 2: Obtain power allocation policy from a mini-batch.
 - 3: Compute the policy gradient of $\mathcal{L}(\mathbf{W}_s, \lambda_s, v_s)$.
 - 4: Update the primal variable \mathbf{W}_s [cf. (??)]:
 $\mathbf{W}_{s+1} = \mathbf{W}_s - \theta_{\mathbf{W},s} \nabla_{\mathbf{W}} \mathbb{E}_{\rho \sim \mathcal{A}} \{\mathcal{L}(\mathbf{W}_s, \lambda_s, v_s)\}$.
 - 5: Update the dual variable λ_s and v_s [cf. (??)-(??)]:
 $\lambda_{s+1} = [\lambda_s + \theta_{\lambda,s} (\mathbb{E}_{\rho \sim \mathcal{A}} \{\log(P_{out,K})\} - \log(\varepsilon))]_+$,
 $v_{s+1} = [v_s + \theta_{v,s} (\mathbb{E}_{\rho \sim \mathcal{A}} \{p_{avg}\} - \bar{p})]_+$.
 - 6: end for
-

IV. Numerical Experiments

Numerical experiments are conducted for verification in this section. For illustration, we assume that $\xi_1 = \dots = \xi_K = 1$, $\delta = 1$, $K = 3$, $R = 2$ bps/Hz, $N_b = 10^6$ bits, $B = 10$ MHz, and $\varepsilon = 10^{-2}$. With regard to the neural network structure, a 5-layer GCN with intermediate feature dimensions 16, 32, 16 and 2 is implemented. The activation functions $\sigma(\cdot)$ in the intermediate layers use “ReLU”, while the last layer applies “Linear”. A dataset with 1000 samples is used in the training stage, the total number of training epochs is set to 500, and the learning rates of $\theta_{\mathbf{W},s}$, $\theta_{\lambda,s}$, and $\theta_{v,s}$ are assumed to be 5×10^{-4} , 10^{-3} and 5×10^{-5} , respectively. The GCN parameters \mathbf{W} are updated by using the adaptive moment estimation (Adam) optimizer. Besides, the expectations in (??) - (??) are taken over the sampled mini-batch of size 50, and ρ is randomly generated from a uniform distribution within the interval $[0, 1)$.

In Fig. ??, the convergence of the primal-dual learning algorithm for three HARQ schemes is investigated by setting $\bar{p} = 15$ dBW. Clearly from Fig. ??, the proposed algorithm can converge within 1200 iterations, which justifies the effectiveness of the GCN-based power allocation strategy. If the maximum power constraint \bar{p} is sufficiently large (e.g., 15 dBW), the LTAT converges to the predefined transmission rate $R = 2$ bps/Hz. Hence, it is observed from Fig. ?? that the latency approaches to $N_b/(B\eta) = 10^6/(10^7 \times 2) = 0.05$ s with the increase of the number of iterations.

In Figs. ?? and ??, the minimal latency and the corresponding outage probability are plotted against the total average transmit power \bar{p} , respectively, where $\rho = 0.5$ is considered. It is not beyond our expectation from both figures that HARQ-IR performs the best, followed by HARQ-CC, and the worst is Type-I HARQ. Moreover, it can be seen from Fig. ?? that a significant latency reduction can be achieved by HARQ-IR under a small \bar{p} when compared to the other two HARQ schemes. In addition, it can be observed from Figs. ?? and ?? that there is no feasible solution for Type-I HARQ and HARQ-CC under a sufficiently low transmit power. However, under

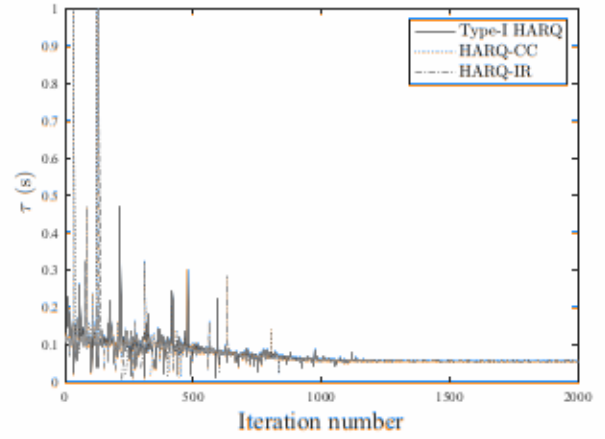


Fig. 3. The convergence analysis of the primal-dual learning algorithm with respect to the number of iterations.

a large power constraint, e.g., $\bar{p} > 16$ dBW, the latency curves of three HARQ schemes almost coincide with each other. Hence, the superior performance of HARQ-IR in terms of the low latency is weakened as \bar{p} increases. Nevertheless, it can be seen from Fig. ?? that HARQ-IR still has a notable outage reduction compared to the other two schemes. Moreover, as \bar{p} increases, the latency is lower bounded by 0.05 s, which has been illustrated in Fig. ?. Whereas, the corresponding outage probabilities of three HARQ schemes continuously decline with \bar{p} .

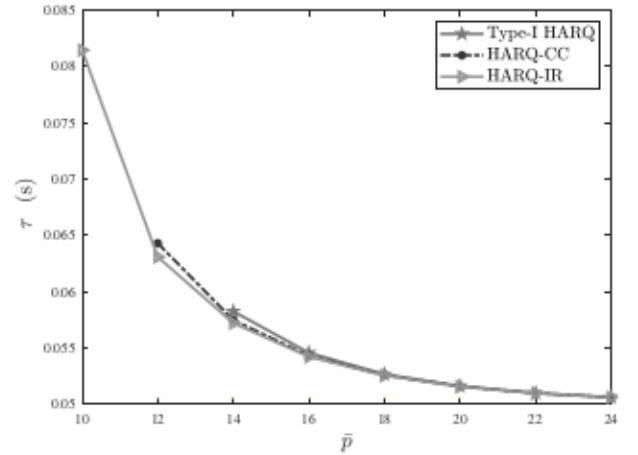


Fig. 4. The comparison between the latency of different HARQ schemes.

As shown in Figs. ?? and ??, the effects of the time correlation on the latency and the outage probability are respectively examined by fixing $\bar{p} = 15$ dBW. It is consistent with the observations in [?], [?], [?] that the time correlation has a negative impact on the latency and outage performance. For example, as the time correlation increases from 0 to 0.98, the latency of HARQ-IR increases from 0.0554 s to 0.0564 s, and the corresponding outage probability of HARQ-IR decreases from 5.76×10^{-5} to